

# Measurement of $tZq$ differential cross-section

Dissertation  
zur  
Erlangung des Doktorgrades (Dr. rer. nat.)  
der  
Mathematisch-Naturwissenschaftlichen Fakultät  
der  
Rheinischen Friedrich-Wilhelms-Universität Bonn

vorgelegt von  
Nilima Akolkar  
aus  
Vadodara, India

Bonn 2023

DRAFT

Angefertigt mit Genehmigung der Mathematisch-Naturwissenschaftlichen Fakultät der Rheinischen  
Friedrich-Wilhelms-Universität Bonn

1. Gutachter: Prof. Dr. John Smith  
2. Gutachterin: Prof. Dr. Anne Jones

Tag der Promotion:  
Erscheinungsjahr:

DRAFT

---

# Contents

---

<b>1</b>	<b>The Standard Model</b>	<b>1</b>
1.0.1	Feynman diagrams . . . . .	2
1.1	The Strong Force . . . . .	2
1.2	The Electroweak theory . . . . .	2
1.3	The Higgs mechanism . . . . .	4
1.4	Physics at the hadron colliders . . . . .	4
<b>2</b>	<b>Signal extraction and Background Estimation</b>	<b>7</b>
2.1	The $tZq$ production . . . . .	7
2.2	The $tZq$ Trilepton Channel . . . . .	7
2.2.1	Event Selection . . . . .	8
2.3	Background processes . . . . .	10
2.4	Monte-Carlo (MC) simulations . . . . .	12
2.5	Data and simulated samples . . . . .	13
2.5.1	Signal sample . . . . .	13
2.5.2	Background samples . . . . .	13
2.6	Systematic Uncertainties . . . . .	13
2.6.1	Instrumental or detector uncertainties . . . . .	14
2.6.2	Theoretical uncertainties . . . . .	15
2.7	Artificial Neural Networks . . . . .	15
<b>A</b>	<b>Useful information</b>	<b>3</b>
	<b>Bibliography</b>	<b>5</b>
	<b>List of Figures</b>	<b>7</b>
	<b>List of Tables</b>	<b>9</b>

DRAFT

---

# Todo list

---

Add figure . . . . .	1
Add and explain an example feynman diagram . . . . .	2
Explain matrix element . . . . .	2
fix the format and label reference . . . . .	3
Lepton universality..because $tZq$ trilepton, decay into muons and electrons equal probability . . . . .	5
branching ratio . . . . .	5
This will be useful when EFT section is written. Make sure the section is referenced . . . . .	7
check what cross-section we are quoting . . . . .	7
Do we talk about other decay channels? . . . . .	8
can i put it after PDF? it is also a part of physic at hadron colliders! . . . . .	12
explain the different weights . . . . .	12
UPDATE THIS AFTER NEW SAMPLE and add info about scales . . . . .	13
Add the detailed DSIDs and everything in the appendix and refer here . . . . .	13

DRAFT

---

## The Standard Model

---

Since many years, physical phenomena occurring around us has shaped our understanding about nature. The Standard Model (SM) of particle physics is a theory that explains almost everything that nature has to offer. It is based on fundamental particles and their interactions being governed by Quantum Field Theories (QFTs).

The Standard Model is divided into spin-1 fermions and spin-0 bosons. The fermions are further divided into leptons and quarks as shown in [FIGURE .](#) Another classification of fermions is into generations. The first generation constitutes  $u$ ,  $d$ ,  $e^-$  and  $\nu_e$  which give rise to matter around us. The second and third generation particles are high energy *siblings* of the first generation particles. These are observed at high energies such as colliders. The SM also considers anti-particles which are clones of particles with opposite quantum numbers.

Add figure

These fermions interact with each other via exchanging bosons which are also called *force-carrier* particles. The massless neutral photon ( $\gamma$ ) is the messenger of the electromagnetic (EM) force which is experienced by charged particles. The underlying QFT is called Quantum Electrodynamics (QED). The electrostatic attraction between charged particles is the low-energy manifestation of QED. Among the SM, all fermions except neutrinos are sensitive to the EM force. The underlying symmetry is the U(1) symmetry.

The strong interaction, mediated by massless gluons, is experienced by particles carrying the so-called colour charge. The physics behind the strong interaction is explained in Quantum Chromodynamics (QCD). Only the quarks can interact via the strong interaction. A peculiar thing in QCD is that the gluons themselves also carry colour charge.

The weak force carriers are  $W^\pm$  and  $Z$ , which unlike  $\gamma$  and gluons, are massive and charged in case of  $W^\pm$ . The weak interaction manifests itself in phenomena such as,  $\beta$ -decay and fusion processes inside the sun. All the SM particles, including the neutrinos, can feel the weak force. Before discussing the electroweak unification, let's dive into the weak interaction. The interaction mediated by  $W^\pm$  and  $Z$  is called charged-current weak interaction and neutral-current weak interaction, respectively. The famous Wu experiment proved that the charged current weak interaction violates parity. The parity violating nature of the weak interaction suggests that the interaction vertex must be different from that of QED and QCD. The weak interaction is described using a  $V - A$  vertex and this fact implies that only left-handed chiral particle states and right-handed chiral antiparticle states can participate in charged-current weak interaction.

The last piece of the SM puzzle is the Higgs boson which is a spin-0 boson. All the particles gain



their mass by Higgs mechanism.

### 1.0.1 Feynman diagrams

Interactions between the SM particles can give rise to various processes. In order to visualise it, a tool called Feynman diagrams is widely used. These diagrams are pictorial representations of the interactions which makes use of straight lines with arrows to show particles and anti-particles. Moreover, curly lines are used to show the boson exchanged between them. The Feynman diagrams are symbolic and have no physical meaning.

Add and explain an example feynman diagram

Explain matrix element

## 1.1 The Strong Force

Electrons and nucleus inside an atom are held together by the electromagnetic force. The same force also exists between protons inside the nucleus causing repulsion. However, there exists a force which is strong enough to overcome repulsion and keep the nucleus together. It is called the strong force or the strong nuclear force. The QFT describing the strong force is called Quantum Chromodynamics (QCD) and the underlying symmetry group is SU(3) described by  $3 \times 3$  matrices. The eight generators of the SU(3) group give rise to eight gluons which are the strong force mediators. The structure of the SU(3) group demands that the wave function of the strongly interacting particle must be a 3-component vector. This gives rise to a new degree of freedom called "colour", with three states called red, blue and green. Consequently, particles having a non-zero colour charge can feel the strong force. Among the SM particles, only quarks have the colour charge which can be either red, blue or green.

A major differentiating factor between QCD and QED is that the gauge boson in QCD carries the charge of interaction. In other words, gluons also carry the colour charge which allows them to interact with other gluons as well. As a result of this self-interaction, no coloured object can be found as a free particle in nature. Due to this so-called colour confinement, quarks cannot exist independently but instead are found in colour-neutral states called *hadrons*. For instance, if two quarks are pulled away from each other, a gluon field is created between them which is proportional to the separation. The gluon fields is so strong that at some point, the energy in this field is sufficient to produce new quarks and antiquarks that form colourless bound states. This process is called hadronisation. Due to colour confinement, only certain configurations for hadrons are permitted. The possible combinations discovered so far can be categorised into mesons ( $q \bar{q}$ ), baryons ( $q q q$ ) and antibaryons ( $\bar{q} \bar{q} \bar{q}$ ).

## 1.2 The Electroweak theory

In the 1960s, physicists were trying to formulate a gauge theory for weak interactions similar to QED. A theory can be a gauge theory if it has an underlying mathematical symmetry and it is renormalisable<sup>1</sup>. Glashow, Salam and Weinberg discovered such a gauge theory by unifying electromagnetic force and the weak force.

---

<sup>1</sup> A quantum field theory is renormalisable if...

The electroweak (EW) theory is a unification of QED and the theory of weak interactions. It is described by the symmetry group  $SU(2)_L \otimes U(1)_Y$ . The corresponding charges of the electroweak theory are the weak isospin  $I, I_3$  and the weak hypercharge  $Y$ . The weak hypercharge  $Y$  determines the interaction under the  $U(1)$  transformations. The weak isospin of particles determines their transformation under  $SU(2)$  and therefore, it is used to make multiplets of particles. The left-handed leptons ( $\ell_L$ ) will form doublets as shown in EQUATION because they transform into each other under the influence of weak force. This is due to the  $V - A$  vertex form of the weak interaction. On the other hand, the right-handed particles are singlets ( $\ell_R$ ).

fix the format and label reference

$$\ell_R = e^-_R, \mu^-_R, \tau_R$$

$$\ell_L = \begin{pmatrix} \nu_e \\ e^- \end{pmatrix}_L, \begin{pmatrix} \nu_\mu \\ \mu^- \end{pmatrix}_L, \begin{pmatrix} \nu_\tau \\ \tau^- \end{pmatrix}_L$$

The Lagrangian of the EW model introduces three bosons  $W_\mu^{(1,2,3)}$  corresponding to  $SU(2)$  and one  $B_\mu$  corresponding to  $U(1)$ . The experimentally observed  $W^\pm$  are combination of  $W_\mu^{(1)}$  and  $W_\mu^{(2)}$  whereas photon ( $A$ ) and the Z-boson are linear combinations of  $W_\mu^{(3)}$  and  $B_\mu$  based on the weak mixing angle ( $\theta_W$ ) as given below:

$$A_\mu = +B_\mu \cos\theta_W + W_\mu^{(3)} \sin\theta_W$$

$$Z_\mu = -B_\mu \sin\theta_W + W_\mu^{(3)} \cos\theta_W$$

The weak interaction for the quark sector can be explained by creating similar  $SU(2)$  doublets (Q).

$$Q = \begin{pmatrix} u \\ d' \end{pmatrix}, \begin{pmatrix} c \\ s' \end{pmatrix}, \begin{pmatrix} t \\ b' \end{pmatrix}$$

The strength of the weak interactions for quarks is determined experimentally by studying nuclear  $\beta$ -decay. It is observed that the vertices corresponding to different quark flavours have different coupling strengths. The reason for this is given by the Cabibbo hypothesis which states that, the flavour eigen states that participate in the weak interactions are a mixture of the mass eigen states. The relation between them is given by the Cabibbo-Kobayashi-Maskawa (CKM) matrix.

$$\begin{pmatrix} d' \\ s' \\ b' \end{pmatrix} = \begin{pmatrix} V_{ud} & V_{us} & V_{ub} \\ V_{cd} & V_{cs} & V_{cb} \\ V_{td} & V_{ts} & V_{tb} \end{pmatrix} \begin{pmatrix} d \\ s \\ b \end{pmatrix}$$

The values of the CKM matrix elements can be found in [1]. The diagonal of the matrix is close to unity, suggesting that the weak interaction is stronger within the same generation of quarks.

The experiments at the Gargamelle bubble chamber in 1973 hinted the evidence of a neutral massive boson responsible for the observed neutrino interactions [2]. In 1983, the Z-boson was directly

discovered at the Super-Proton Synchrotron at CERN. The electroweak theory was verified by this pathbreaking discovery. The properties of the Z-boson were studied at the Large Electron-Positron (LEP) collider at CERN. The discovery of Z and W bosons are among the crucial tests of the Standard Model.

### 1.3 The Higgs mechanism

### 1.4 Physics at the hadron colliders

#### Parton Distribution Functions(PDFs)

Protons at the LHC collide at high energies giving rise to deep inelastic interactions called hard processes. In such cases, the interactions are not between protons but between their constituents which are quarks and gluons, collectively known as *partons*. These partons carry a fraction of the total momentum of the proton (or a hadron in general). In order to study an interaction, it is important to know the effective energy of the interacting partons and their flavour. This information is encoded in the Parton Distribution Functions (PDFs). It describes the probability of finding a parton of certain flavour  $i$ , carrying a momentum fraction  $x_i$  at a certain energy scale.

#### Pileup

At the LHC 2808 bunches of protons are injected which are 25 ns apart. This results into  $1.2 \times 10^{11}$  protons per bunch giving rise to different particle interactions. The primary hard scatter collisions, that are of interest, are contaminated by soft interactions called pileup. It is defined by the average number of interactions recorded per bunch crossing. Sources of pileup are categorized into in-time and out-of-time pileup. In-time pile up is due to collisions occurring in the same bunch-crossing and out-of-time pile-up is contributed by the collisions from previous or later bunches. Some of the sub-detectors have sensitivity windows longer than the interval between bunch crossings. This eventually affects the recorded number of interactions per bunch. The accurate detection of objects under study becomes difficult due to pile-up events. The higher the luminosity, more the pileup. The object reconstruction algorithms have dedicated procedures to mitigate pileup.

#### Luminosity and cross-section ( $\sigma$ )

The quantity that measures the ability of a collider to produce particle interactions is called instantaneous luminosity ( $\mathcal{L}$ ). The instantaneous luminosity integrated over the lifetime of collider operation is called integrated luminosity ( $L$ ).

In order to define the event rate for interesting processes, along with luminosity, we require another quantity called the cross-section. At the subatomic scale, the particle interactions are governed by laws of quantum physics. Therefore, a theory can predict the *probability* of certain outcomes of collisions. The probability that a certain process will take place is called its cross-section ( $\sigma$ ). Finally, the number of event rate of specific interactions is defined as the product of integrated luminosity and the cross-section (Eq. (1.1)).

$$R = \sigma \cdot \int_{dt} \mathcal{L}(t) \quad (1.1)$$

For a particle collider, beam energies and the luminosity are two important figures of merit. High energy allows the production of new heavy particles and high luminosity allows more flux of particles contributing to high number of collisions.

The outcomes of these collisions hold interesting physics and it is studied with the help of particle detectors. The LHC houses four main detectors at the four collision points. The two general purpose detectors are ATLAS (A Toroidal LHC ApparatuS)[3] and CMS (Compact Muon Solenoid)[4]. The LHCb experiment[5] is dedicated to studies based on  $B$ -hadron and its decays whereas ALICE(A Large Ion Collider Experiment)[6] analyses the  $Pb-Pb$  collisions at the LHC. This analysis uses data from the ATLAS detector which is described in the next section.

Lepton universality..because  $t \rightarrow Zq$  tripleton, decay into muons and electrons equal probability

branching ratio



## Signal extraction and Background Estimation

### 2.1 The $tZq$ production

High energy proton-proton collisions at the LHC enable multiple processes to occur simultaneously. Out of those processes, the process of interest for this analysis is the electroweak production of the  $t$ -quark and the  $Z$ -boson, referred to as the  $tZq$  production. The LO  $t$ -channel Feynman diagrams are shown in Fig. 2.1 where a  $Z$ -boson can be radiated from any one of the incoming or outgoing quarks (Fig. 2.1(a)) or from the exchanged  $W$ -boson (Fig. 2.1(b)). In addition to these resonant contributions, there is also a small non-resonant contribution in the form of  $tl^+l^-q$  (Fig. 2.1(c)) which is also accounted for. The  $t$ -quark can be produced through interactions such as  $u + b \rightarrow d + Z + t$  or  $\bar{u} + b \rightarrow \bar{d} + Z + t$  whereas  $\bar{t}$ -quark can be produced via charge conjugate processes. The NLO QCD corrections for  $tZq$  are small and therefore any possible deviations from the SM can be studied in the context of SM Effective Field Theory.

This will be useful when EFT section is written. Make sure the section is referenced

The  $tZq$  production probes the coupling of  $t$  and  $Z$  as well as the  $WWZ$  coupling. Hence, it allows the coupling of two bosons and the coupling of a fermion to a boson to be studied in a single interaction. Moreover, it can provide a solid basis to study similar processes such as the  $tHq$  process. The expected cross-section of the  $tZq$  production in the SM, calculated at NLO in QCD for a dilepton mass more than 30 GeV, is  $(102^{+5}_{-2})$  fb. The cross-section, measured by the ATLAS collaboration, is  $(97 \pm 13 \text{ (stat.)} \pm 7 \text{ (sys.)})$  fb which is consistent with the SM expectation.

check what cross-section we are quoting

In order to study this process, one has to note that the particles involved are quite heavy and therefore, the only way to spot them is from their reconstructed decay products. Conventionally, the possible final states are divided into several *channels* based on certain combinations of leptons and jets. This analysis focuses on the so-called trilepton channel as described below.

### 2.2 The $tZq$ Trilepton Channel

As the name suggests, the trilepton decay channel of the  $tZq$  production contains final states with three charged leptons, as shown in Fig. 2.2. The  $t$ -quark decays almost exclusively into  $b W$  and the corresponding  $W$  decays into a charged lepton and an associated neutrino. The  $Z$ -boson decays into

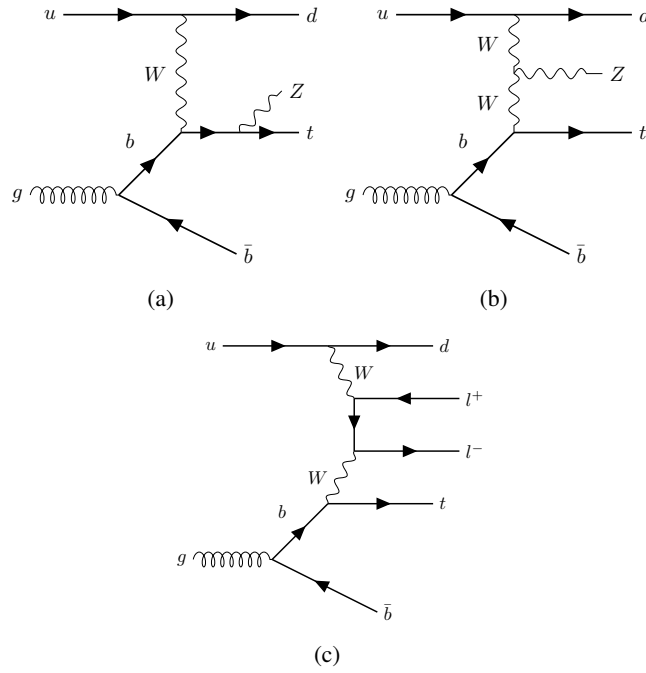


Figure 2.1: Feynman diagrams at LO for the  $tZq$ -production. The  $Z$  is radiated either from one of the quarks or from the exchanged  $W$  boson.

opposite sign same flavour lepton pairs and its probability is equal across the three lepton families ( $e^-$ ,  $\mu^-$ ,  $\tau^-$ ) due to lepton universality. This analysis includes  $Z$  decays resulting into electrons or muons ( $e^- e^+$  or  $\mu^- \mu^+$ ). The  $\tau^-$ -leptons are considered if they decay into lighter leptons (i.e.  $e^-$  or  $\mu^-$ ).

Do we talk about other decay channels?

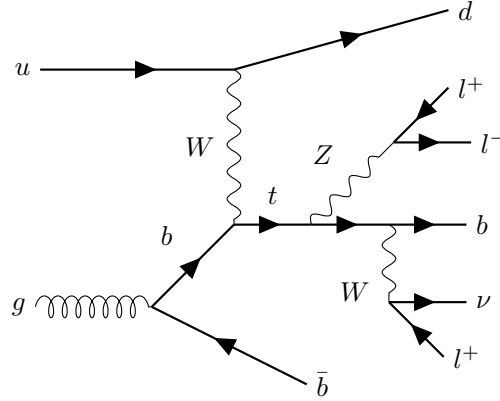
The branching ratio of the trilepton channel is relatively small. However, it has a clean signature due to the three lepton requirement. In addition, three lepton final state is quite difficult to mimic by background processes. This is the reason to choose this final state for studying  $tZq$  process. For this analysis, the trilepton final state is referred to as the signal.

### 2.2.1 Event Selection

The next task is to reconstruct this final state from the detector data or in other words, find possible occurrences of this final state within the collision events. In order to achieve that, certain requirements are defined in favour of the signal events. The collection of these requirements is called event selection. For this analysis, the primary event selection is discussed below and summarised in Table 2.1.

- **Leptons**

- Exactly three leptons ( $e^-$  or  $\mu^-$ ),  $\tau$  is considered if it decays into leptons. These leptons are sorted by their  $p_T$  which is required to be at least 27, 15 and 10 GeV, respectively.

Figure 2.2: The  $tZq$  trilepton final state

- At least 1 Opposite Sign Same Flavour (OSSF) lepton pair with a minimum difference between its invariant mass ( $m_{ll}$ ) and  $m_Z$ . This is to identify which out of the selected leptons originate from  $Z$ .
- A cut on minimum accepted invariant mass, in order to suppress backgrounds not containing a  $Z$ .
- A cut on the transverse mass of the  $W$ -boson is applied to account for the missing transverse energy.

#### • Jets

- Number of jets are required to be between 2 and 5, with  $p_T$  more than 25 GeV and  $|\eta|$  more than 4.5.
- Number of  $b$ -jets are required to be 1 or 2, reconstructed at 85% working point with  $|\eta|$  more than 2.5. Events with 2 jets, both  $b$ -tagged are not considered.

Table 2.1: Event selection

Variable	Preselection
$N_\ell$ ( $\ell = e, \mu$ )	$= 3$
	$\geq 1$ OSSF lepton pair
$p_T(\ell_1, \ell_2, \ell_3)$	$> 27, 15, 10$ GeV
$\min(m_{\ell\ell})$	$> 20$ GeV
$ m_{\ell\ell} - m_Z $	$< 10$ GeV
$m_T(\ell, E_T^{\text{miss}})$	$> 30$ GeV
$N_{\text{jets}}(p_T > 25 \text{ GeV})$	2-5
$N_{b\text{-jets}} @ 85\%$	1-2 (no $2j2b$ )

It is important to note here that these requirements are chosen to maximise the probability of selecting signal events but in reality there are background processes that mimic the  $tZq$  signature and therefore, contaminate the selected signal events.



## 2.3 Background processes

The background processes for  $tZq$  process can be classified according to the number of prompt (or real) leptons in the final state. A lepton is labelled prompt if it originates from either a  $\tau$  or a massive boson. On the other hand, non-prompt or fake leptons are objects misidentified as leptons. The source of non-prompt leptons can be bottom and charm hadron decays, meson decays, photon conversions or light jets creating lepton-like signatures. Backgrounds involving only prompt leptons are diboson,  $t\bar{t}+X$ ,  $t\bar{t}H$  and  $tWZ$  while backgrounds involving non-prompt leptons are  $t\bar{t}$ ,  $Z$  +jets and  $tW$ .

### Backgrounds involving prompt leptons

In the diboson process, two massive bosons are produced which can be  $ZZ$ ,  $WW$  or  $WZ$ , as shown in Fig. 2.3. As per Fig. 2.3(a), the leptonic decay of bosons result into three prompt leptons which can pass the signal event selection if additional jets are also found. For the  $ZZ$  scenario, as shown in Fig. 2.3(b), one of the leptons needs to fail the requirement for a prompt lepton or is not reconstructed. Due to this strong resemblance of the diboson signature with the signal, it is the dominant background in the  $tZq$  production.

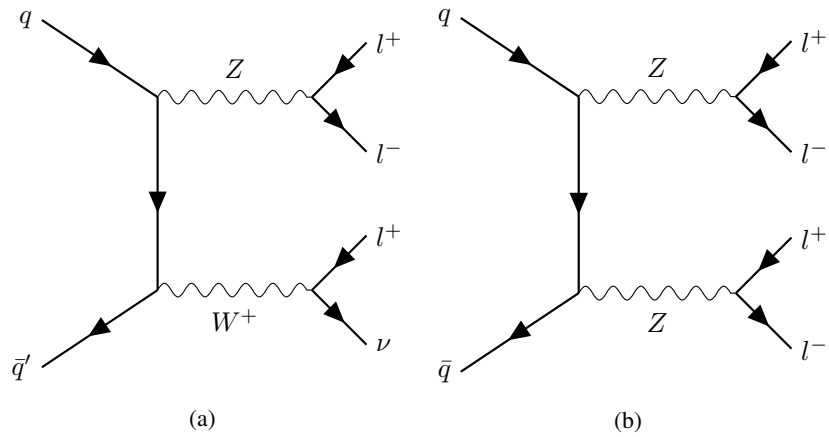


Figure 2.3: Feynman diagrams for the diboson background

The  $t$ -quark pair production in association with a heavy boson ( $Z$  or  $W$ ) can be an important source of background. In particular, the  $t\bar{t}Z$  process, where the final state already includes a  $Z$  boson and a  $t$  quark, can produce a very similar signal-like signature. It is shown in Fig. 2.4. The  $t\bar{t}H$  contributes less because of its small cross-section.

### Backgrounds involving non-prompt leptons

Backgrounds involving non-prompt or fake lepton are  $t$ -quark pair production and the production  $Z$ -boson with jets. As shown in Fig. 2.5(b), there are already two leptons from the  $Z$ -boson. If the jets are light, they can be misidentified as leptons leading to a non-prompt lepton contribution. In the  $t\bar{t}$  production, as shown in Fig. 2.5(b), if one of the  $b$ -jet decays into a lepton, then it can satisfy the signal event selection.

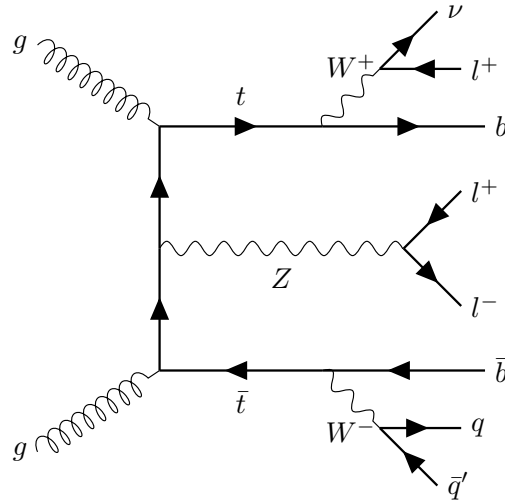


Figure 2.4: Feynman diagrams for the  $t\bar{t}Z$  background

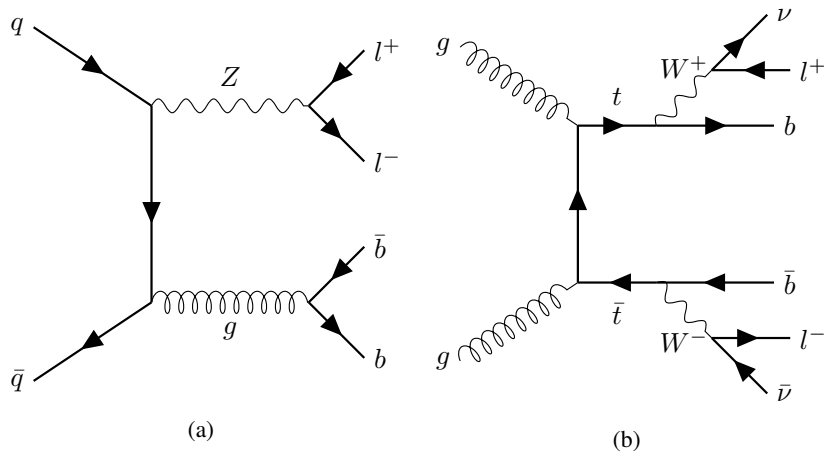


Figure 2.5: Feynman diagrams for non-prompt lepton background

## 2.4 Monte-Carlo (MC) simulations

can i put it after PDF? it is also a part of physic at hadron colliders!

As already discussed before, proton-proton collisions are viewed as collisions between partons. This is not a simple process because multiple interactions can occur within the same event. With this complexity, it becomes difficult to study the interaction of interest and more importantly the task of segregating signal from background becomes more complex. Here is where, Monte Carlo generators come to the rescue. Monte Carlo generators are software that simulate collision events along with detector effects and try to provide a detailed description of the possible final states. More precisely, they use pseudo-random numbers to reproduce the quantum mechanical probabilities of different outcomes of a collision event [7].

The simulated data provided by these generators can be thought of as a "digital twin" of the actual observed data. It can be used to predict any experimental observable or a combination of observables. The MC chain is a step-by-step process that begins with identifying the hard interaction and continues until the final state is achieved. At each stage, the structure of the underlying event evolves. The steps are briefly summarised below:

- **Hard process:** In this step the hard process, defined as the process with highest momentum transfer, is determined using matrix element calculation combined with the input Parton Distribution Functions. If a resonance is produced in a hard process, such as the  $t$  or  $Z$  and it shortly decays, then its decay process is also considered within the hard process.
- **Parton Shower (PS):** The colliding partons are responsible for emissions that give rise to more partons and subsequently more interactions. The emissions associated with the incoming partons is called Initial-State Radiation (ISR) while the emissions associated with outgoing partons is called Final-State Radiation (FSR). These emissions and their respective interactions are modelled with Parton Shower algorithms. The incorporation of PS into the matrix element paints a more accurate picture of the collision process.
- **Multiple-processes:** Until now, only one of the partons from the original hadron is considered but in reality, other partons from the same hadron also interact. Their interactions are termed as multiple-processes and they are calculated at this step of the MC simulation chain.
- **Hadronisation and decay:** The outgoing partons, with sufficient energy, can produce new hadrons due to QCD colour confinement (hadronisation). If these hadrons are unstable, they can also decay into lighter particles. The MC chain also includes these calculations.

Finally, detector simulation is applied, after which the simulated data is ready for comparison with the detector data. Among the various available MC generators, HERWIG [8] and PYTHIA [9] are two of the most commonly used ones.

explain the different weights

## 2.5 Data and simulated samples

This analysis uses collision data collected by the ATLAS detector during 2015 to 2018 (Run-2 of the LHC) at a center of mass energy of 13 GeV. The total integrated luminosity is of  $140.1 \text{ fb}^{-1}$ .

The ATLAS MC samples for analysis of the Run-2 dataset are divided into three subsets: mc16a generated with 2015 and 2016 pileup conditions, mc16d generated with 2017 pileup conditions and mc16e that includes pileup conditions of 2018 data.

### 2.5.1 Signal sample

The  $tZq$  signal sample is simulated using MADGRAPH5\_AMC@NLO 2.9.5 generated at next-to-leading order (NLO) with NNPDF3.0NLO parton distribution function. In general, the models used for PS and hadronisation contain several free parameters which must be optimised to generate a reasonable description of data. The optimisation is termed as tuning and the resulting sets of parameters are called tune sets. For the signal sample, PYTHIA 8.245 is used for Parton Shower and hadronisation along with A14 (ATLAS 24 [10]) tune set and the NNPDF2.3LO PDF set. The  $t$ -quark is decayed at LO using MADSPIN.

UPDATE THIS AFTER NEW SAMPLE and add info about scales

### 2.5.2 Background samples

For the background processes, different versions of MADGRAPH5\_AMC@NLO [11], SHERPA [12] or POWHEG [13] generators are used to calculate the matrix element and cross-sections combined with the NNPDFx.xNLO PDF set. The PS and hadronisation is modeled with PYTHIA for the nominal background samples and HERWIG for the alternate sample generation. The alternate samples are required for the theoretical uncertainties as described in SECTION. The specific versions used for different backgrounds is summarised in Table 2.2.

Add the detailed DSIDs and everything in the appendix and refer here

## 2.6 Systematic Uncertainties

One of the key advantages of using simulated data is their ability to predict how the observed data may appear. However, it is crucial to assess how dependable both the simulated and the measured data are, which is quantified through uncertainties. The proper inclusion of uncertainties is an important part of any analysis.

Uncertainties can be divided into two sections: statistical and systematic. Simply put, statistical uncertainties are related to the statistics of the data whereas systematic uncertainties are complex uncertainties that are not directly from the statistics of the data. For instance, the length of an object is measured with a ruler and is found to be  $10 \pm 0.5 \text{ cm}$ . Here the statistical uncertainty is 0.5 cm. In addition, there is a systematic uncertainty which can originate from the calibration of the ruler.

In high energy physics, sources of systematic uncertainties are calibrations of scales, efficiencies of particle identifications and reconstructions, choice of MC generators, etc. These sources of

Table 2.2: Background sample details

Background	Generator	Parton Shower	PDF	Type of Sample
$t\bar{t}Z$	MADGRAPH5_AMC@NLO 2.8.1	PYTHIA 8.244	NNPDF3.0NLO NNPDF2.3LO	Nominal
$t\bar{t}Z$	MADGRAPH5_AMC@NLO 2.8.1	HERWIG 7.2.1	NNPDF3.0NLO NNPDF2.3LO	Alternate
$tWZ$	MADGRAPH5_AMC@NLO 2.X.X	PYTHIA 8.235	NNPDF3.0NLO	Nominal
Diboson	SHERPA 2.2.12	SHERPA MEPS@NLO	NNPDF3.0NNLO	Nominal
Triboson	SHERPA 2.2.2	SHERPA MEPS@NLO	NNPDF3.0NNLO	Nominal
$t\bar{t}$	POWHEG BOX v2	PYTHIA 8.230	NNPDF3.0NLO NNPDF2.3LO	Nominal
$t\bar{t}$	HERWIG 7.2.1	PYTHIA 8.230	NNPDF3.0NLO	Alternate
$tW$	POWHEG BOX v2	PYTHIA 8.230	NNPDF3.0NLO NNPDF2.3LO	Nominal
$Z$ + jets	SHERPA 2.2.11	SHERPA MEPS@NLO	NNPDF3.0NNLO	Nominal
$t\bar{t}W$	SHERPA 2.2.10	SHERPA MEPS@NLO		Nominal
$t\bar{t}H$	POWHEG BOX v2	PYTHIA 8.230	NNPDF3.0NLO NNPDF2.3LO	Nominal
$t\bar{t}t$	MADGRAPH5_AMC@NLO 2.2.2	PYTHIA 8.186	NNPDF2.3LO	Nominal
$t\bar{t}\bar{t}$	MADGRAPH5_AMC@NLO 2.3.3	PYTHIA 8.230	NNPDF3.1LO	Nominal
$t\bar{t}t\bar{t}$	MADGRAPH5_AMC@NLO 2.3.3	HERWIG 7.0.4	NNPDF3.1LO	Alternate

systematic uncertainties are categorised into: instrumental and theoretical uncertainties as described in Section 2.6.1 and Section 2.6.2, respectively.

### 2.6.1 Instrumental or detector uncertainties

- **Luminosity:** The integrated luminosity is  $140.1 \text{ fb}^{-1}$  and the uncertainty in its calculation is 0.83%
- **Pileup reweighting:** MC generators make use of scale factors to account for differences in pileup distributions between data and simulations. There is an uncertainty associated with these scale factors. It is evaluated by changing the nominal pileup value to a lower and a higher value, then the effect of these changes is calculated to obtain the up and down uncertainty.
- **Jet Energy Scale (JES):** After the jets are reconstructed, their energies need to be adjusted so that it reflects the energy of the colliding particles. The calibration is done by comparing the reconstructed jets with the true jets which are simulated jets of stable particles without detector effects. Uncertainties originating from the calibration process are categorised as JES uncertainties [14].
- **Jet Energy Resolution (JER):** JER is the detector's ability to distinguish two jets with similar total energy. The uncertainty associated with the differences in JER in case of data and simulation is called JER uncertainty.
- **Lepton reconstruction:** Scale factors are applied to correct differences between data and simulation in case of lepton identification, isolation and trigger efficiencies. The uncertainties associated with these scale factors belong to the lepton reconstruction category of systematics.

### 2.6.2 Theoretical uncertainties

- **MC Modeling uncertainties:** This category involves uncertainties originating from the various models used in the MC simulation chain.

The uncertainty associated with the A14 tune set is determined by comparing the nominal sample with two alternate samples, both simulated using the same settings as the nominal sample but incorporating the up and down variations of the A14 tune set. This variation is related to the strong coupling constant  $\alpha_s$ .

## 2.7 Artificial Neural Networks

A neural network is a computation tool developed to function in a way similar to the human mind. It is widely used in high energy physics for data analysis. The structure of a neural network (NN) is made up of neurons or *nodes*. Their function is to examine unknown systems and identifying interesting features, just like the job of neurons in human mind. Generally, these nodes are arranged in three different layers: the input layer, the hidden layer and the output layer. A list of variables is given as input to the nodes of the input layer. Processing takes place through the subsequent layers and at the end, the output layer returns the conclusions derived by the network. Connections between nodes of different layers are referred to as the *synapses*. Each connection between nodes of two consecutive layers, has a weight associated to it.

The input received by each node is the sum of weighted output of all nodes of the previous layer. As given in Equation 2.1,  $y_j$  is the input to node  $j$ ,  $w_{ij}$  is the weight from the  $i$ -th node and  $x_i$  is that node's output. The term  $w_{0j}$  is called bias.

$$y_j = \sum_{i=1}^n w_{ij}x_i + w_{0j} \quad (2.1)$$

The output of a node is defined by an *activation* function. Common choice of an activation function is the sigmoid function. It provides output between 0 and 1. A feature that makes a NN special is its capability to *learn* from examples with known inputs and outputs. This is referred to as *training* a neural network. The purpose of training is to find appropriate weights. In supervised training, inputs and outputs are provided to a NN. It processes input and then compares the resultant output with the desired output. Comparison is done by calculating a *loss function*. It is a way to determine how well is the network trained. For better performance of a network the loss function should be minimised. In order to do that, errors of the resultant output are propagated back in a model and the initial weights are readjusted so that output is closer to the desired output. This is how a network learns. A dataset flows inside a network several times and each time weights are refined until a minimum value of the loss function is obtained.



---

## Bibliography

---

- [1] S. N. et al. (Particle Data Group), Phys. Rev. D 110, 030001 (2024),  
URL: <https://pdg.lbl.gov/2024/api/index.html> (cit. on p. 3).
- [2] F. Hasert et al., *Observation of neutrino-like interactions without muon or electron in the gargamelle neutrino experiment*, Physics Letters B **46** (1973) 138, ISSN: 0370-2693,  
URL: <https://www.sciencedirect.com/science/article/pii/0370269373904991>  
(cit. on p. 3).
- [3] *The ATLAS Experiment at the CERN Large Hadron Collider*,  
Journal of Instrumentation **3** (2008) S08003,  
URL: <https://dx.doi.org/10.1088/1748-0221/3/08/S08003> (cit. on p. 5).
- [4] *The CMS experiment at the CERN LHC*, Journal of Instrumentation **3** (2008) S08004,  
URL: <https://dx.doi.org/10.1088/1748-0221/3/08/S08004> (cit. on p. 5).
- [5] *The LHCb Detector at the LHC*, Journal of Instrumentation **3** (2008) S08005,  
URL: <https://dx.doi.org/10.1088/1748-0221/3/08/S08005> (cit. on p. 5).
- [6] *The ALICE experiment at the CERN LHC*, Journal of Instrumentation **3** (2008) S08002,  
URL: <https://dx.doi.org/10.1088/1748-0221/3/08/S08002> (cit. on p. 5).
- [7] T. Sjöstrand, *Monte Carlo Generators*,  
2006 European School of High-Energy Physics, ESHEP 2006 (2006) (cit. on p. 12).
- [8] J. Bellm et al., *Herwig 7.0/Herwig++ 3.0 release note*,  
The European Physical Journal C **76** (2016) 196,  
URL: <https://doi.org/10.1140/epjc/s10052-016-4018-8> (cit. on p. 12).
- [9] T. Sjöstrand, S. Mrenna and P. Skands, *A brief introduction to PYTHIA 8.1*,  
Computer Physics Communications **178** (2008) 852, ISSN: 0010-4655,  
URL: <https://www.sciencedirect.com/science/article/pii/S0010465508000441>  
(cit. on p. 12).
- [10] *ATLAS Pythia 8 tunes to 7 TeV data*, tech. rep., All figures including auxiliary figures are  
available at <https://atlas.web.cern.ch/Atlas/GROUPS/PHYSICS/PUBNOTES/ATL-PHYS-PUB-2014-021>; CERN, 2014, URL: <https://cds.cern.ch/record/1966419>  
(cit. on p. 13).
- [11] J. Alwall et al., *The automated computation of tree-level and next-to-leading order differential cross sections, and their matching to parton shower simulations*, JHEP **07** (2014) 079,  
arXiv: [1405.0301](https://arxiv.org/abs/1405.0301) [hep-ph] (cit. on p. 13).



- [12] T. Gleisberg et al., *Event generation with SHERPA 1.1*,  
*Journal of High Energy Physics* **2009** (2009) 007,  
URL: <https://dx.doi.org/10.1088/1126-6708/2009/02/007> (cit. on p. 13).
- [13] A. Banfi et al., *A POWHEG generator for deep inelastic scattering*, *JHEP* **02** (2024) 023,  
arXiv: 2309.02127 [[hep-ph](#)] (cit. on p. 13).
- [14] T. Barillari and O. behalf of the ATLAS Collaboration,  
*Jet Energy Scale Uncertainties in ATLAS*,  
*Journal of Physics: Conference Series* **404** (2012) 012012,  
URL: <https://dx.doi.org/10.1088/1742-6596/404/1/012012> (cit. on p. 14).

---

## List of Figures

---

2.1	Feynman diagrams at LO for the $tZq$ -production . . . . .	8
2.2	The $tZq$ trilepton final state . . . . .	9
2.3	Feynman diagrams for diboson backgrounds . . . . .	10
2.4	Feynman diagrams for the $t\bar{t}Z$ background . . . . .	11
2.5	Feynman diagrams for non-prompt lepton backgrounds . . . . .	11



---

## List of Tables

---

2.1	Event selection . . . . .	9
2.2	Background sample details . . . . .	14